MOLECULAR AND CELLULAR BIOLOGY, Sept. 2006, p. 6609–6622 Vol. 26, No. 17
0270-7306/06/$08.00+0 doi:10.1128/MCB.00295-06

Mice with a Targeted Mutation of *Patched2* Are Viable but Develop Alopecia and Epidermal Hyperplasia†

Erica Nieuwenhuis,[1,2] Jun Motoyama,[1,3] Paul C. Barnfield,[1,2] Yoshiaki Yoshikawa,[1,4] Xiaoyun Zhang,[1] Rong Mo,[1] Michael A. Crackower,[1,2,5] and Chi-chung Hui[1,2]*

Program in Developmental Biology, The Hospital for Sick Children,[1] and Department of Molecular and Medical Genetics,[2] University of Toronto, Toronto Medical Discovery Towers, 101 College Street, Toronto, Ontario M5G 1L7, Canada; Molecular Neuropathology Group, Brain Research Institute, RIKEN, 2-1 Hirosawa, Wako, Saitama 351-0198, Japan[3]; Department of Dermatology, Tenri Hospital, 200 Michimo-cho, Tenri-shi, Nara 632-8552, Japan[4]; and Department of Biochemistry and Molecular Biology, Merck Frosst Centre for Therapeutic Research, Montreal, Quebec H3R 3P8, Canada[5]

Received 16 February 2006/Returned for modification 15 April 2006/Accepted 16 June 2006

Hedgehog (Hh) signaling plays pivotal roles in tissue patterning and development in *Drosophila melanogaster* and vertebrates. The *Patched1* (*Ptc1*) gene, encoding the Hh receptor, is mutated in nevoid basal cell carcinoma syndrome, a human genetic disorder associated with developmental abnormalities and increased incidences of basal cell carcinoma (BCC) and medulloblastoma (MB). *Ptc1* mutations also occur in sporadic forms of BCC and MB. Mutational studies with mice have verified that *Ptc1* is a tumor suppressor. We previously identified a second mammalian *Patched* gene, *Ptc2*, and demonstrated its distinct expression pattern during embryogenesis, suggesting a unique role in development. Most notably, *Ptc2* is expressed in an overlapping pattern with *Shh* in the epidermal compartment of developing hair follicles and is highly expressed in the developing limb bud, cerebellum, and testis. Here, we describe the generation and phenotypic analysis of $Ptc2^{tm1/tm1}$ mice. Our molecular analysis suggests that $Ptc2^{tm1}$ likely represents a hypomorphic allele. Despite the dynamic expression of *Ptc2* during embryogenesis, $Ptc2^{tm1/tm1}$ mice are viable, fertile, and apparently normal. Interestingly, adult $Ptc2^{tm1/tm1}$ male animals develop skin lesions consisting of alopecia, ulceration, and epidermal hyperplasia. While functional compensation by *Ptc1* might account for the lack of a strong mutant phenotype in *Ptc2*-deficient mice, our results suggest that normal *Ptc2* function is required for adult skin homeostasis.

The Hedgehog (Hh) family of secreted signaling molecules plays critical roles in embryonic patterning and organ development in *Drosophila melanogaster* and vertebrate species. Many components of the Hh signaling pathway were first identified in *Drosophila*, and recent studies have revealed both evolutionarily conserved and divergent aspects of the pathway (17, 31, 48, 49). In both *Drosophila* and vertebrate cells, two transmembrane proteins, Patched (Ptc) and Smoothened (Smo), are involved in the reception of Hh signals. Ptc inhibits the signaling activity of Smo when Hh is absent, and binding of Hh to Ptc relieves the inhibition on Smo, resulting in the transcriptional activation of Hh target genes. Vertebrates possess two *Patched* genes, *Ptc1* and *Ptc2*. In humans, *Ptc1* is a tumor suppressor gene mutated in nevoid basal cell carcinoma syndrome (NBCCS), which is characterized by various developmental anomalies and a predisposition to develop basal cell carcinoma (BCC) and medulloblastoma (MB) (25). Furthermore, *Ptc1* mutations are also found in sporadic forms of BCC and MB. $Ptc1^{+/-}$ mice display a mutant phenotype similar to those observed in NBCCS patients and develop tumors, including MB and skin tumors (5, 24, 27, 28).

Ptc encodes a receptor protein containing 12 hydrophobic membrane-spanning domains, intracellular amino- and carboxy-terminal regions, and two large hydrophilic extracellular loops, where Hh ligand binding occurs (29, 40, 60). Responsiveness of cells to Hh can be abolished by mutating or deleting the extracellular domains of Ptc (11, 47). The Ptc receptor belongs to a family of integral-membrane proteins that characteristically possess a sterol-sensing domain (SSD), which is implicated in vesicle trafficking (35); however, the role of the SSD of Ptc in Hh signaling remains unclear. In *Drosophila*, Ptc and Hh colocalize to intracellular vesicles in Hh-responding cells, suggesting that the Hh-Ptc complex is internalized upon binding (10, 12, 41, 61). Similarly, in mammalian cells, Sonic hedgehog (Shh) can be internalized by cells transfected with Ptc1, followed by targeting of both proteins to the lysosome (42). These findings support a model of Ptc-mediated endocytosis for regulating the availability of the ligand. Internalization of Ptc and Ptc1 can occur via dynamin-dependent endocytosis mediated by clathrin-coated pits (13, 30). Caveolin, a major coat protein of caveolae, has also been identified as a Ptc-binding partner, suggesting that non-clathrin-coated plasma membrane invaginations (caveolae) may be involved in the endocytosis and trafficking of Ptc (32).

The precise mechanism by which Ptc regulates Smo is unclear. A catalytic model for Ptc function has been proposed (62); the levels of free Ptc (unbound by Hh) determine the degree of pathway activity as well as the amount of Hh ligand required for stimulation of the pathway (62). Ptc shows simi-

* Corresponding author. Mailing address: Program in Developmental Biology, The Hospital for Sick Children, Toronto Medical Discovery Towers, MaRS Building, East Tower, Room 13-314, Toronto, Ontario M5G 1L7, Canada. Phone: (416) 813-5681. Fax: (416) 813-5252. E-mail: cchui@sickkids.ca.

† Supplemental material for this article may be found at http://mcb.asm.org/.

larity to the resistance, nodulation, division (RND) family of bacterial proton gradient-driven transmembrane molecular transporters. In bacteria, RND proteins are responsible for removing antibiotics, toxic organic compounds, and metal ions from cells (64). Therefore, like other RND proteins, Ptc might function as a molecular transporter. In addition, the intracellular loop of Ptc has been shown to interact with cyclin B1, resulting in inhibition of cell proliferation by mediating the localization of phosphorylated cyclin B1 (9).

Most studies on *Ptc* function focus on *Ptc1*, and very little is known about the role of *Ptc2* in development. We have previously identified the mouse *Ptc2* gene and shown that it displays overlapping expression with *Shh* during epidermal development in mouse embryos (46). Mouse *Ptc2* is located at mouse chromosome 4C7-D1 (23), which is syntenic to human chromosome 1p36-31.3, where multiple tumor suppressor genes have been mapped (45). Reverse transcription-PCR (RT-PCR) analysis revealed *Ptc2* expression in the adult mouse brain, stomach, intestine, kidney, heart, lung, and liver. RNA in situ hybridization analysis also detected *Ptc2* expression in primary and secondary spermatocytes of adult mouse testes (14). Similar to Ptc1, Ptc2 also contains 12 transmembrane domains and two large extracellular loops, but, different from Ptc1, Ptc2 possesses much shorter amino- and carboxy-terminal regions.

Both *PTCH1* (57, 58) and *PTCH2* (52) were shown to generate several splice variants. In *PTCH2* alternative splicing appears to affect mostly the C-terminal region and the sterol-sensing domain (52).

Biochemical studies revealed that human PTCH1 and PTCH2 bind to all Hh family members (Sonic hedgehog, Desert hedgehog [Dhh], and Indian hedgehog [Ihh]) with similar affinities (14). Since *Ptc2* is highly expressed in the testis, it has been suggested that it acts as the receptor for Dhh, which is required for germ cell development (14). Recently, it was suggested that the Dhh-Ptc2 signaling pathway is involved in the maintenance of adult nerves where *Ptc2*, but not *Ptc1*, is expressed in peripheral nerve cells. Interestingly, *Ptc2* and *Dhh* expression was upregulated in regenerating nerves, suggesting that Ptc2 is the major receptor of Dhh in adult nerves (8). In addition, PTCH2 splice variants were able to reconstitute a Dhh-dependent transcriptional response in cells lacking *Ptc1* function (52). It was reported that Ptc2 and *Ihh* are highly expressed in equine osteochondrosis-affected cartilage and repair tissue, suggesting that Ihh-Ptc2 signaling might play a role in diseased adult cartilage (56).

PTCH2 mutations have been detected in some cases of sporadic BCC and MB, suggesting that it might play a role in tumorigenesis (58). Interestingly, like *PTCH1*, *PTCH2* is highly expressed in both familial and sporadic BCC (66) and MB (36), indicating that *Ptc2* is a target gene of Shh signaling in the skin and that *Ptc2* may be under negative regulation by *Ptc1*.

Murine hair follicle development begins at embryonic day 14 (E14), when the mesenchyme instructs the overlaying ectoderm to form an epidermal placode. In response the placode signals to mesenchymal fibroblasts to form a dermal condensate. The dermal condensate responds by instructing follicular keratinocytes to proliferate and differentiate into the mature follicle. During follicular development, *Shh* is required for proliferation: in $Shh^{-/-}$ embryos hair follicle development is arrested (59), while overexpression of *Shh* (K14-*Shh*) results in hyperproliferative basaloid lesions developing at the expense of hair follicles (1, 50). Postnatal follicles cycle through successive phases of anagen (active growth), catagen (regression), and telogen (resting), and Shh acts as a biological switch instructing hair follicles to enter anagen (55).

To determine the role of *Ptc2* in mammalian development, we generated a targeted mutant allele, $Ptc2^{tm1}$, by homologous recombination in embryonic stem (ES) cells. Our analysis suggests that $Ptc2^{tm1}$ is likely a hypomorphic allele of *Ptc2*. We present here a phenotypic analysis of $Ptc2^{tm1/tm1}$ mice. Our results indicate that $Ptc2^{tm1/tm1}$ mice develop normally, are viable and fertile, and do not display any obvious defects in hair follicle, limb, neural, or testis development. However, $Ptc2^{tm1/tm1}$ male mice develop skin lesions with progressing age consisting of alopecia (hair loss) and epidermal hyperplasia, suggesting a role for *Ptc2* in adult epidermal homeostasis.

MATERIALS AND METHODS

Gene targeting of Ptc2. A *Ptc2* clone was isolated from an Sv/129 mouse genomic library for the construction of the targeting vector, which contains a 2.0-kb XhoI-XhoI fragment and a 4.5-kb XhoI-BamHI fragment flanking the *phosphoglycerol kinase-neo* cassette (Fig. 1A). A herpes simplex virus *thymidine kinase* gene was inserted next to the longer arm and used for negative selection. The targeting vector was confirmed by restriction analysis and DNA sequencing. Mouse R1 ES cells were electroporated with the vector and subjected to positive selection with G418 and negative selection with ganciclovir. Targeted ES cell clones were identified by Southern blot analysis, and two independent *Ptc2* mutant clones were used to generate germ line chimeras by embryo aggregation. F1 animals were verified by Southern blot hybridization using a 700-bp DNA fragment as indicated in Fig. 1A. Mice heterozygous for the *Ptc2* mutant allele ($Ptc2^{tm1/+}$ mice) were interbred to generate $Ptc2^{tm1/tm1}$ mice. PCR genotyping was performed on ear punch specimens using a combination of three primers, WT1 (5′-CCTGGCCCACCTGTGCCTTA-3′), WT2 (5′-GACCTTCACTAACCTCAGGC-3′), and Neo (5′-TTCCATTTGTCACGTCCTGCACG-3′), to amplify a 150-bp wild-type fragment and a 350-bp mutant fragment (Fig. 1B).

Northern analysis. Poly(A)$^+$ RNA from mouse testis was prepared using an Oligotex kit (QIAGEN) according to the manufacturer's instructions. Three micrograms of RNA was separated on an agarose formaldehyde gel and transferred onto a nitrocellulose membrane (Genescreen). A *Ptc2* cDNA probe was labeled with [α-^{32}P]dCTP using Ready-To-Go DNA-labeling beads (Amersham).

RT-PCR analysis. Total RNA was extracted from mouse testis, skin, and cerebellum using Trizol (Invitrogen) according to the manufacturer's instructions. RT-PCRs were performed using the Superscript one-step RT-PCR kit (Invitrogen) and the following primers: Ptc2-AF (5′-GTCTCCGAGTGGCTGTAA-3′), Ptc2-AR (5′-TTCTCAATCATCCGTTCG-3′), Ptc2-BF (5′-CACCCCCGAGGCACTTGA-3′), Ptc2-BR (5′-GCCCCGGAAGTGCTCGTA-3′), Ptc2-CF (5′-GTGGCTCCCCCTTCCTCTTCT-3′), Ptc2-CR (5′-AGGGGCAAAGGTCTGTTCC-3′), GAPDH-F (5′-GTGGCAAAGTGGAGATTGTTGCC-3′), GAPDH-R (5′-GATGATGACCCGTTTGGCTCC-3′), Ptc1-F (5′-AACAAAAATTCAACCAAACCTC-3′), Ptc1-R (5′-TGTCTTCATTCCAGTTGATGTG-3′), Gli1-F (5′-TTCGTGTGCCATTGGGGAGG-3′), and Gli1-R (5′-CTTGGGCTCCACTGTGGAGA-3′). Reaction conditions are available upon request. The intensity of *Ptc1* and *Gli1* amplification products was analyzed and compared to the internal control (*GAPDH*), using ImageJ software. *Ptc2* transcripts were subcloned into a TA vector (Invitrogen), and the products were examined by DNA sequencing.

Generation of myc-tagged Ptc2 expression constructs. Template cDNA was generated from wild-type testes RNA (Superscript first-strand synthesis system for RT-PCR; Invitrogen). Overlapping primers were designed to amplify *Ptc2* cDNA lacking the start codon (AccuPrime *Pfx* DNA polymerase; Invitrogen). Based on sequencing information obtained regarding *Ptc2* mutant transcripts (see above) primers were designed to amplify the affected regions (exons 1 to 4, 1 to 5, 7 to 12, and 8 to 12). Products were verified by sequencing and assembled in a pcDNA3.1 vector (Invitrogen) modified by in-frame insertion of an N-terminal myc cassette (ATGCAAAAACTCATCTCAGAAAGAGGATCTG). The following constructs were generated: Ptc2-WT, Ptc2-Δ5,6, Ptc2-Δ6, and Ptc2-Δ6,7. Primers and reaction conditions are available upon request.

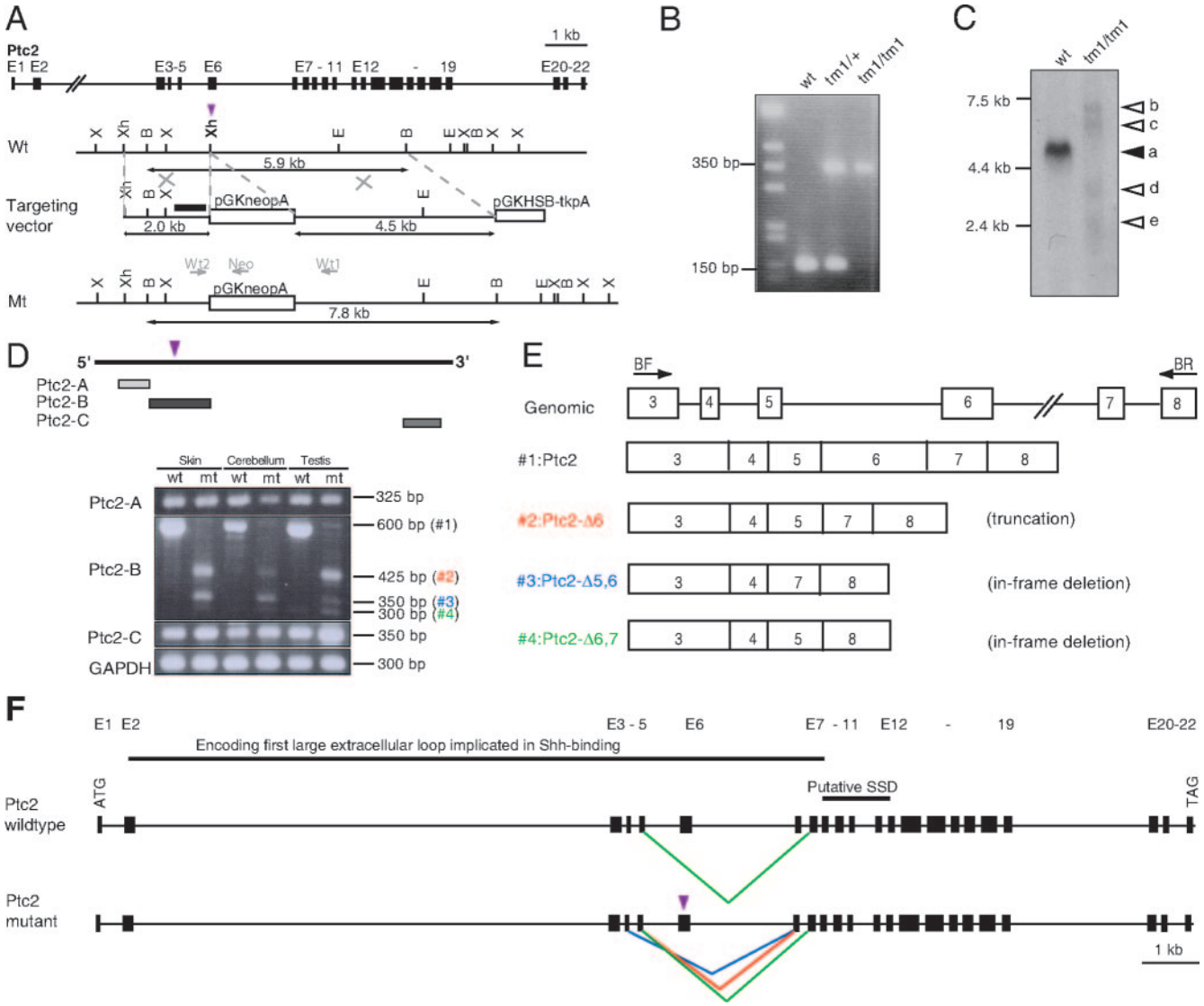

FIG. 1. Disruption of *Ptc2* by gene targeting. (A) Targeting strategy illustrating the genomic organization, a restriction map of the wild-type (Wt) locus, the targeting vector, and the targeted allele (Mt). *Ptc2* is located in chromosome 4 and consists of 22 predicted exons. The black bar indicates the position of the probe used for Southern hybridization. Arrows indicate positions of genotyping primers. X, XbaI; Xh, XhoI; B, BamHI; E, EcoRI. (B) Genotyping of progeny by PCR analysis. PCR amplification generated wild-type (150-bp) and mutant (350-bp) bands. (C) Northern blot analysis. The major transcript (a) encoded by *Ptc2* is absent in $Ptc2^{tm1/tm1}$ testis RNA. Four transcripts (b to e), ranging from 2.4 to 7.5 kb, are present in $Ptc2^{tm1/tm1}$ testis RNA. (D) RT-PCR analysis of *Ptc2* expression in skin, cerebellum, and testis of wild-type and mutant mice. The diagram indicates the locations of primer pairs Ptc2-A (325 bp), Ptc2-B (600 bp), and Ptc2-C (350 bp) relative to the insertion (arrowhead). Similar results were obtained for all transgenic tissues analyzed. Ptc2-A and Ptc2-C amplified fragments of the expected sizes in wild-type and *Ptc2* mutant samples. Ptc2-B amplified expected transcript 1 in the wild type only, transcripts 2 and 3 in the mutant only, and transcript 4 present in the wild type and mutant. (E) Schematic representation of sequencing results obtained for wild-type and mutant transcripts amplified by Ptc2-B primers. Arrows indicate locations of forward (BF) and reverse (BR) primers relative to the genomic sequence. Three alternative splice forms of *Ptc2* were isolated, with deletions of exon 6, exons 5 and 6, and exons 6 and 7. (F) Schematic depicting the location of alternative splice forms present in *Ptc2* mutants. The translational start ATG codon resides in exon 1. The putative first extracellular loop, implicated in interacting with Shh, is encoded by exons 2 to 9, while the putative sterol-sensing domain is encoded by exons 9 to 13. Our targeting strategy aimed at disrupting the first large extracellular loop of Ptc2, thereby abolishing its interaction with Shh. Ptc2-Δ6,7 represents an alternative splice form of *Ptc2* in which exons 6 and 7 are deleted, resulting in an in-frame deletion. In the *Ptc2* mutant, two additional splice forms are generated, Ptc2-Δ6 and Ptc2-Δ5,6.

Confocal microscopy and immunofluorescence. CH310T1/2 cells were maintained in Dulbecco's modified Eagle medium supplemented with 10% fetal bovine serum. Cells were seeded on gelatin-treated coverslips and transfected using Fugene6 (Roche). At 48 h posttransfection, cells were fixed, followed by incubation with anti-c-myc (Santa Cruz) or antihemagglutinin (HA; Santa Cruz). Slides were processed for indirect fluorescence (fluorescein isothiocyanate-conjugated secondary antibody; Jackson Laboratories) visualization.

Luciferase assays. $Ptc1^{-/-}$ embryonic fibroblasts were maintained as previously described (6). 8xGli-BS-luc (54) reporter assays were performed as previously described (18) following transfection of Ptc1-HA (6), Ptc2-myc, Ptc2-Δ5,6-

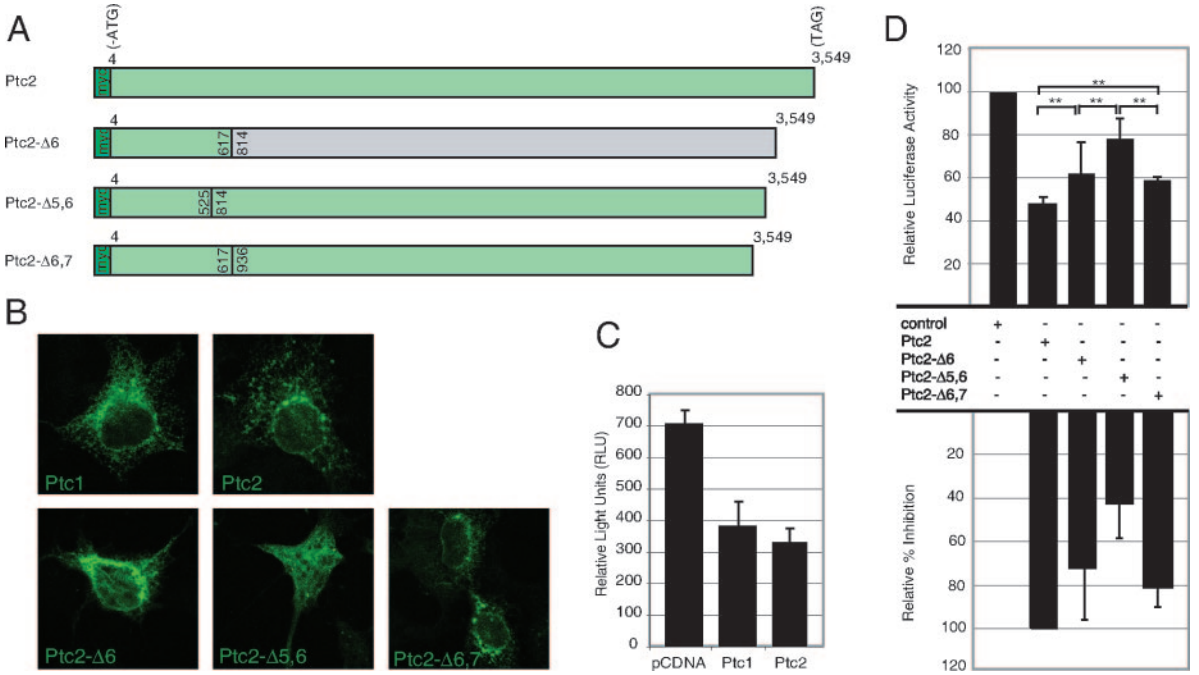

FIG. 2. In vitro analysis of Ptc2 mutant forms. (A) Schematic indicating myc-tagged expression constructs for wild-type and mutant Ptc2. Deletion of exon 6 in Ptc2-Δ6 likely results in a premature truncation of the Ptc2 protein (gray shading). (B) Subcellular localization of Ptc1, Ptc2 wild-type, and Ptc2 mutant constructs. Ptc2-Δ5,6 is present in the cytoplasmic and nuclear compartments, while Ptc2-Δ6 and Ptc2-Δ6,7 are localized similarly to Ptc1 and Ptc2. (C) Luciferase assay showing that Ptc2 can function similarly to Ptc1 as a negative regulator of Shh signaling. The data shown are the averages from three independent experiments performed in triplicate. (D) Graph showing the effect of Ptc2 mutant forms on Gli-dependent transcription represented as relative luciferase activity and relative % inhibition. When compared to wild-type Ptc2, each of the mutants showed a statistically significant increase in Gli-dependent transcription (**, $P < 0.05$). Ptc2-Δ6 and Ptc2-Δ6,7 behaved similarly, and the differences in their relative luciferase activities were not statistically significant. Ptc2-Δ5,6 had the greatest decrease in its ability to inhibit Gli-dependent transcription compared to Ptc2. The results are from two independent experiments performed in triplicate.

myc, Ptc2-Δ6-myc, or Ptc2-Δ6,7-myc expression constructs. Gli-dependent transcription was measured and normalized using a dual-luciferase reporter assay (Promega). Data were obtained from three independent experiments, each performed in triplicate, for Fig. 2C and two independent experiments, each performed in triplicate, for Fig. 2D.

Histological and skeletal analyses. Embryos at E15.5 and E18.5 from heterozygous intercrosses were collected and fixed in 4% (wt/vol) paraformaldehyde (PFA) in phosphate-buffered saline (PBS) overnight at 4°C, processed, and embedded in paraffin following standard procedures. Dorsal and front paw skin samples from adult wild-type, heterozygous, and homozygous mutant animals were also processed. For histological analysis, 5-μm sections were prepared and stained with hematoxylin and eosin. Skeletal analysis of E18.5 embryos was performed using alcian blue/alizarin red bone staining (44).

In situ hybridization. Tissues and embryos were fixed in 4% PFA in PBS for 16 h at 4°C. Paraffin sections (5 μm) or whole-mount embryos were subjected to in situ hybridization with digoxigenin-dUTP-labeled riboprobes as described previously (19). Plasmids used for generating riboprobes were those carrying *Ptc1*, *Gli1*, *Shh* (46), *Keratin-15* (B. Morgan), *Keratin-17* (P. Coulombe), and *Ptc2-N* (generated by RT-PCR; nucleotides 504 to 827).

Immunohistochemistry. Immunohistochemistry was carried out as described previously (16) on 5 μm paraffin sections. Dilutions and other details concerning antibodies are available upon request. The following primary antibodies were used: keratin-5, keratin-14, keratin-10, loricrin (Covance), cyclin D1/D2, PCNA, phospho-histone H3 (Ser10) (Cell Signaling Technology), and GATA-3 (Santa Cruz). Fluorescein isothiocyanate- or tetramethyl rhodamine isocyanate-conjugated (Jackson Laboratories), as well as biotinylated (Vector Labs), secondary antibodies were used, followed by visualization with the ABC Vectastain and VIP or NovaRed color substrate kits (Vector Labs). Endogenous alkaline phosphatase activity was detected using rehydrated paraffin sections. Sections were equilibrated in APB buffer (0.1 M NaCl, 0.05 M MgCl, 0.1 M Tris, pH 9.5, 0.1% Tween 20) for 45 min, followed by a 2-hour incubation with BM Purple (Roche) at room temperature in the dark. Following immunohistochemistry, sections were dehydrated and mounted using Permount. Sections were examined and photographed using an Axioskop microscope (Carl Zeiss).

RESULTS

Targeted disruption of *Ptc2*. To investigate the role of *Ptc2* in mammalian development, we generated $Ptc2^{tm1/tm1}$ mice. The *Ptc2* gene was disrupted in ES cells by targeted insertion of a *neomycin* resistance cassette (pGKNeopA) in exon 6 (Fig. 1A), which encodes part of the large extracellular loop of the Ptc2 protein (Fig. 1F), implicated in direct interaction with Shh (29, 40). This modification was expected to result in a loss-of-function mutant allele due to several stop codons created 3′ to the insertion. Germ line chimeras were obtained from two independently targeted ES cell lines, and both lines gave rise to fertile heterozygous mutant mice. Intercrosses of heterozygous mutant mice were used to generate homozygous mutant mice. Southern blot hybridization confirmed the disruption of the *Ptc2* gene (data not shown). Northern blot analysis revealed that the 5-kb *Ptc2* transcript is absent in the testes of $Ptc2^{tm1/tm1}$ animals (Fig. 1C). Instead, several mutant transcripts ranging from 2.4 to 7.5 kb were detected. We performed RT-PCR on skin, cerebellum, and testis, followed by sequence analyses to further characterize the *Ptc2* mutant transcripts (Fig. 1D and E; see Fig. S1 in the supplemental material). Regions 5′ and 3′ to the insertion were still transcribed from the mutant allele

(products Ptc2-A and Ptc2-C in Fig. 1D). However, using Ptc2-B primers, the 600-bp wild-type transcript was found to be absent in the $Ptc2^{tm1/tm1}$ sample (Fig. 1D, #1). Instead, three mutant transcripts were detected. In wild-type samples, the intensity of the 600-bp transcript was greater than the intensities of any of the transcripts in the mutant. All the mutant transcripts were sequenced. Transcripts 2 and 3 have deletions of exon 6 and exons 5 and 6, respectively. Transcript 4 lacks exons 6 and 7 (Fig. 1E; see Fig. S1 in the supplemental material) and appears to be a minor splice product of *Ptc2* present in both wild-type and $Ptc2^{tm1/tm1}$ RNA. A summary of Ptc2 products generated is presented in Fig. 1E and F; see also Fig. S1 in the supplemental material.

We were unable to determine whether $Ptc2^{tm1}$ is a protein-null allele since attempts to generate a Ptc2-specific antibody were unsuccessful. Instead we generated myc-tagged expression constructs for wild-type and mutant Ptc2 (summarized in Fig. 2A) and performed an in vitro analysis. Ptc1, Ptc2, Ptc2-Δ6, and Ptc2-Δ6,7 appeared to be localized perinuclearly, while Ptc2-Δ5,6 showed diffuse cytoplasmic and nuclear staining (Fig. 2B). Luciferase assays were performed to determine the effect of Ptc2 mutant forms on Gli-dependent transcription (Fig. 2C and D). First we showed that Ptc2 acts similarly to Ptc1 to decrease Gli-dependent transcription (Fig. 2C) when expressed in $Ptc1^{-/-}$ embryonic fibroblast cells. Having established the assay, we examined the mutant forms of Ptc2. We found that, when compared with wild-type Ptc2, Ptc2-Δ5,6 had greatly reduced inhibitory activity, whereas the activities of Ptc2-Δ6 and Ptc2-Δ6,7 were compromised to a lesser extent (Fig. 2D). We consistently observed great variability in the results obtained for Ptc2-Δ6. This mutant form is predicted to be a protein truncated at amino acid 206. Interestingly, Ptc2-Δ5,6, in addition to having lost its ability to negatively regulate Shh signaling, also has altered subcellular localization compared to Ptc2, Ptc2-Δ6, and Ptc2-Δ6,7. Western blot analysis suggested that Ptc2-Δ5,6 is deficient in protein maturation, indicating that the deleted exons might be encoding domains necessary for early folding or glycosylation of Ptc2 (data not shown). *Ptc1* missense mutations in regions encoding the large extracellular loop have previously been shown to affect glycosylation of Ptc1 when overexpressed in $Ptc1^{-/-}$ cells (7). Together, these results suggest that $Ptc2^{tm1}$ likely represents a hypomorphic allele of *Ptc2*.

Normal Ptc2 function is not required for viability. To determine whether *Ptc2* is required during development, we analyzed offspring from $Ptc2^{tm1/+}$ intercrosses. PCR genotyping at 3 weeks of age ($n = 158$) revealed normal Mendelian ratios of $Ptc2^{+/+}$ (22%, $n = 35$), $Ptc2^{tm1/+}$ (54%, $n = 86$), and $Ptc2^{tm1/tm1}$ (23%, $n = 37$) mice, indicating that normal *Ptc2* function is not essential for embryogenesis or postnatal survival. Breeding of male and female $Ptc2^{tm1/tm1}$ mice resulted in healthy offspring, suggesting that *Ptc2* is not required for reproduction. Furthermore, $Ptc2^{tm1/tm1}$ mice did not exhibit any differences in mortality when compared with $Ptc2^{tm1/+}$ or $Ptc2^{+/+}$ control littermates. Thus, normal *Ptc2* function is not required for embryonic development, viability, and fertility.

Normal limb development in Ptc2 mutant mice. *Ptc2* is highly expressed in the posterior mesenchyme of the developing limb buds and can be induced by *Shh* (37, 51). To investigate whether *Ptc2* plays a role in Shh signaling during limb development, we examined the expression of two *Shh* target genes, *Ptc1* and *Gli1*, in $Ptc2^{tm1/tm1}$ mice by whole-mount RNA in situ hybridization (Fig. 3A to H). Consistent with the notion that *Ptc2* may act negatively in Shh signaling, E11.5 $Ptc2^{tm1/tm1}$

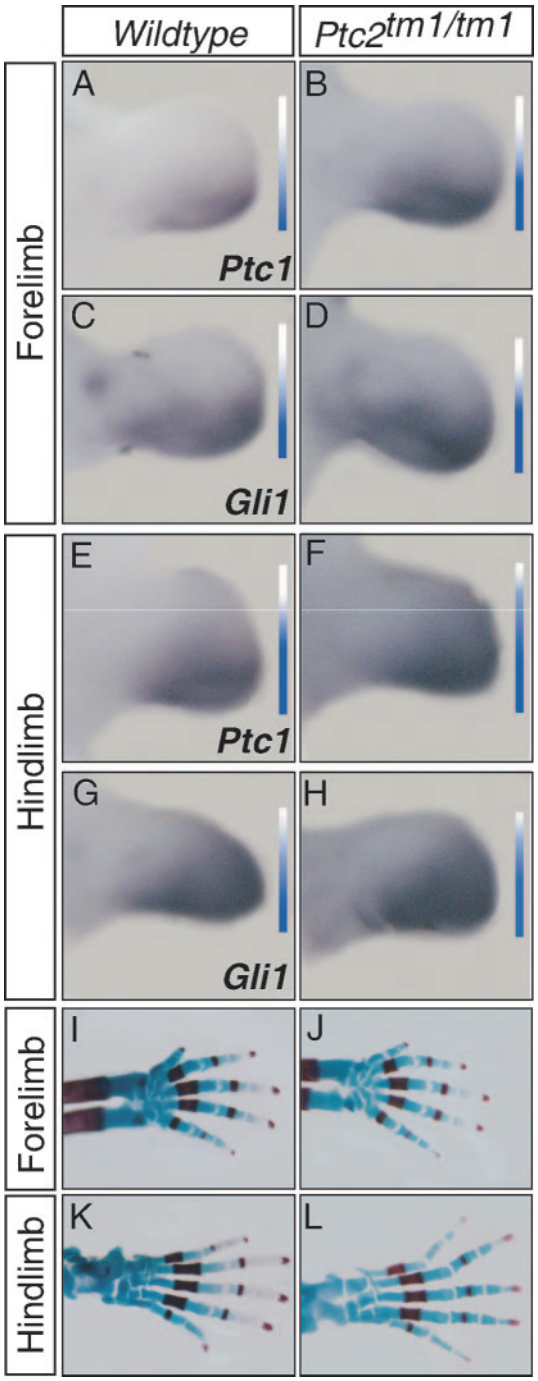

FIG. 3. Normal limb development in *Ptc2*-deficient mice. (A to H) Whole-mount in situ hybridization of E11.5 limb buds. Expression of *Ptc1* (A, B, E, and F) and *Gli1* (C, D, G, and H) in forelimb (A to D) and hind limb (E to H) buds of wild type (A, C, E, and G) and $Ptc2^{tm1/tm1}$ (B, D, F, and H) embryos is shown. Bars containing graded shading indicate increased expression of *Ptc1* and *Gli1* in $Ptc2^{tm1/tm1}$ forelimb and hind limb buds. (I to L) Alcian blue and alizarin red staining of E18.5 wild-type and $Ptc2^{tm1/tm1}$ limbs revealed no significant difference in skeletal patterning and development.

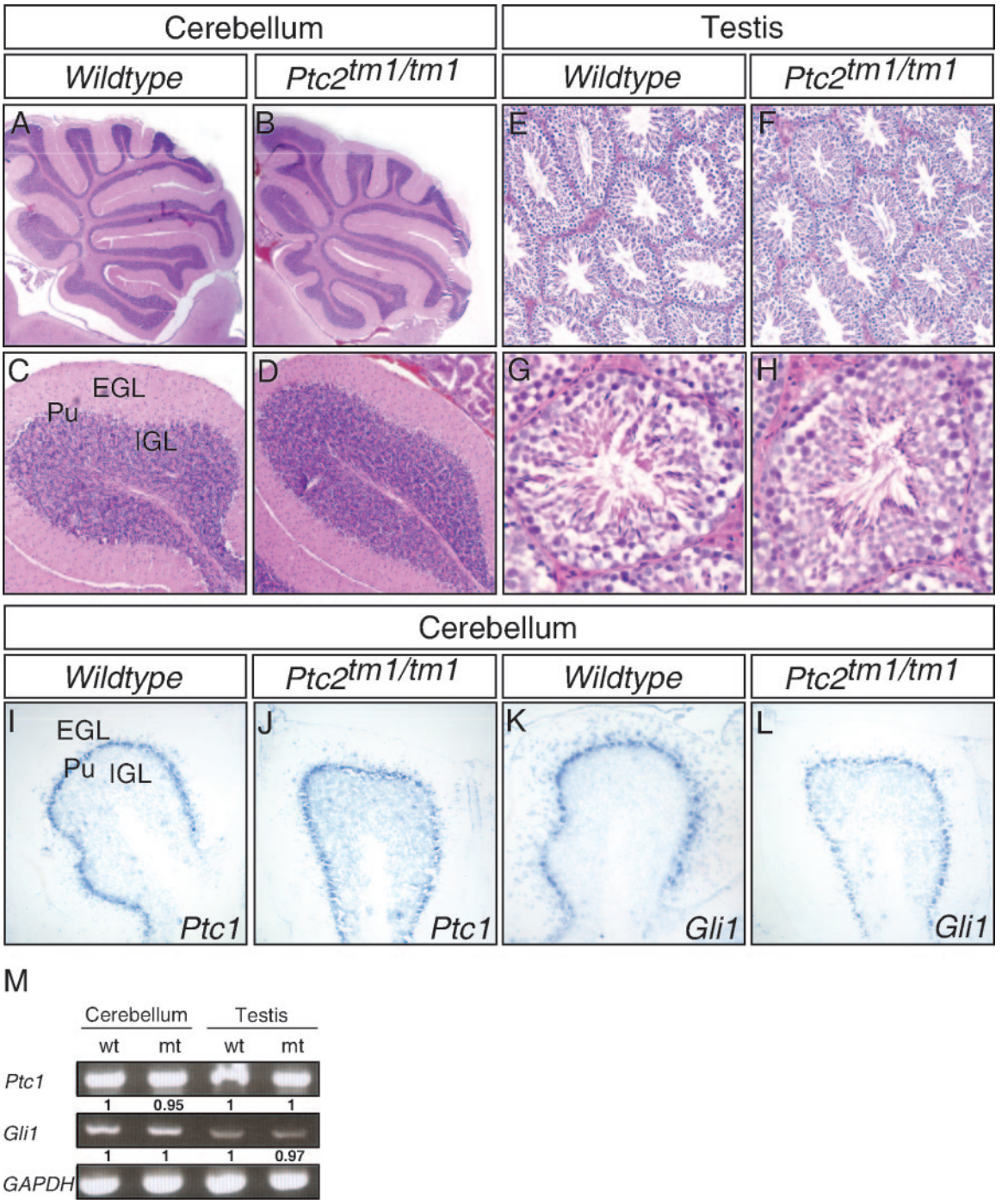

FIG. 4. *Ptc2*-deficient mice develop normal cerebellums and testes, and Ptc1 and Gli1 are not upregulated. Histological staining of cerebellums (A to D) and testes (E to H) of adult wild-type (A, C, E, and G) and *Ptc2*$^{tm1/tm1}$ (B, D, F, and H) mice is shown. (A, B, E, and F) Low-magnification views; C, D, G, H, and I to L, high-magnification views. (I to L) In situ hybridization of *Ptc1* (I and J) and *Gli1* (K and L) showing normal expression in *Ptc2* mutants. IGL, Internal germinal layer; Pu, Purkinje cell layer. (M) Semiquantitative RT-PCR analysis of *Ptc1* and *Gli1* expression levels in wild-type (wt) and *Ptc2*$^{tm1/tm1}$ (mt) cerebellum and testis. Results obtained from RT-PCR analysis were normalized to *GAPDH* (internal control) and are represented as expression detected in wild-type samples compared to mutant samples.

mutant limb buds showed a slight anterior expansion of *Ptc1* and *Gli1* expression. Despite the expansion of *Shh* target gene expression, alcian blue and alizarin red staining of E18.5 skeletons did not reveal any abnormalities in *Ptc2*$^{tm1/tm1}$ mice (Fig. 3I to L), suggesting that reduced *Ptc2* function does not perturb limb patterning and development.

Ptc2 mutants have normal cerebellum and testis development. Both *Ptc1* and *Ptc2* are expressed in the developing

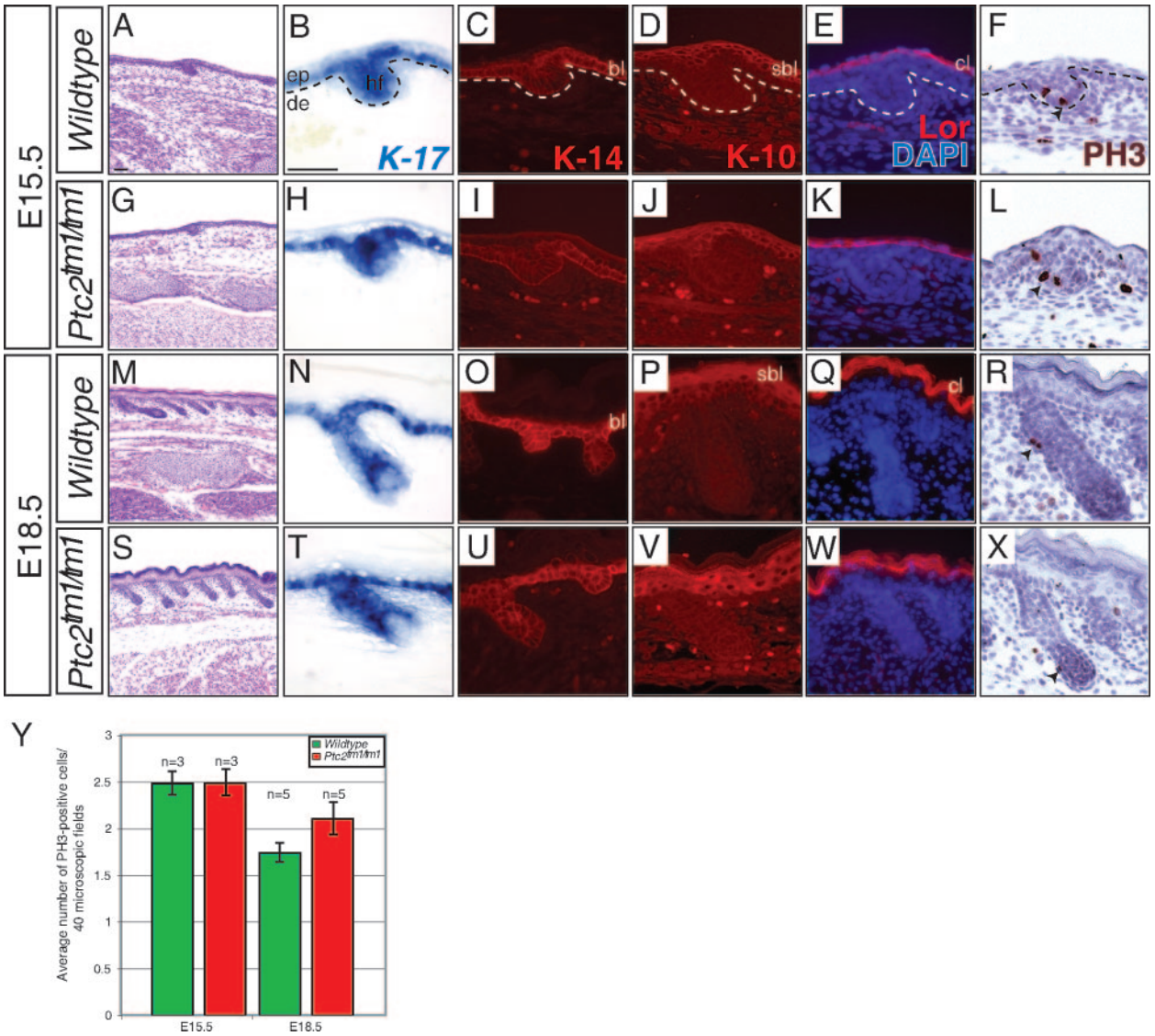

FIG. 5. *Ptc2* is not required for embryonic hair follicle development. Histological analysis of wild-type (A and M) and $Ptc2^{tm1/tm1}$ (G and S) hair follicle development at E15.5 (A and G) and E18.5 (M and S) revealed normal differentiation and proliferation. In situ hybridization and immunohistochemistry for markers of hair follicle development at E15.5 and E18.5 are shown. Expression levels of *Keratin-17* (B, H, N, and T), keratin-14 (C, I, O, and U), keratin-10 (D, J, P, and V), loricrin (E, K, Q, and W), and phospho-histone H3 (PH3) (F, L, R, and X) appear to be normal in the $Ptc2^{tm1/tm1}$ epidermis. (Y) Cell proliferation is not affected in $Ptc2^{tm1/tm1}$ skin at E15.5 or E18.5. Data represent the average numbers of PH3-positive cells (arrowheads in panels F, L, R, and X) obtained from counting 40 contiguous microscopic fields per sample. The error bars indicate standard deviations, and a *t* test revealed that the differences are not statistically significant. Dashed lines indicate epidermis-dermis boundaries. ep, epidermis; de, dermis; bl, basal layer; sbl, suprabasal layer; cl, cornified layer. Scale bar: 50 μM.

cerebellum, but *Ptc2* expression is more restricted and is confined to the proliferative region of the external germinal layer (EGL) at postnatal day 7. This suggests a selective involvement of *Ptc2* in proliferative populations of the EGL (36). However, examination of gross morphology as well as histological analysis did not reveal any abnormalities in the adult *Ptc2* mutant cerebella (Fig. 4A to D). In situ hybridization analysis indicated that *Ptc1* and *Gli1* are not upregulated in $Ptc2^{tm1/tm1}$ cerebella (Fig. 4I to L). Another major site of *Ptc2* expression is the primary and secondary spermatocytes in the seminiferous tubules of the adult testes (14). Since primary and secondary spermatocytes are in close contact with supporting Sertoli cells, which express *Dhh*, it is possible that Ptc2 may act as a receptor for Dhh in the testes. However, *Ptc2* mutant males are fertile and histological analysis of $Ptc2^{tm1/tm1}$ testis did not reveal any abnormalities (Fig. 4E to H). Similar to what was found for cerebella, expression of *Ptc1* and *Gli1* was unaffected in the testes of *Ptc2* mutants (data not shown). Semiquantitative RT-PCR analysis of *Ptc1* and *Gli1* mRNA levels (Fig. 4M) confirmed results obtained by in situ hybridization. Together, these results indicate that normal *Ptc2* function is not required for the development of the cerebellum or testes.

Ptc2 is not required for embryonic hair follicle development. Shh signaling is essential for the development of epidermal

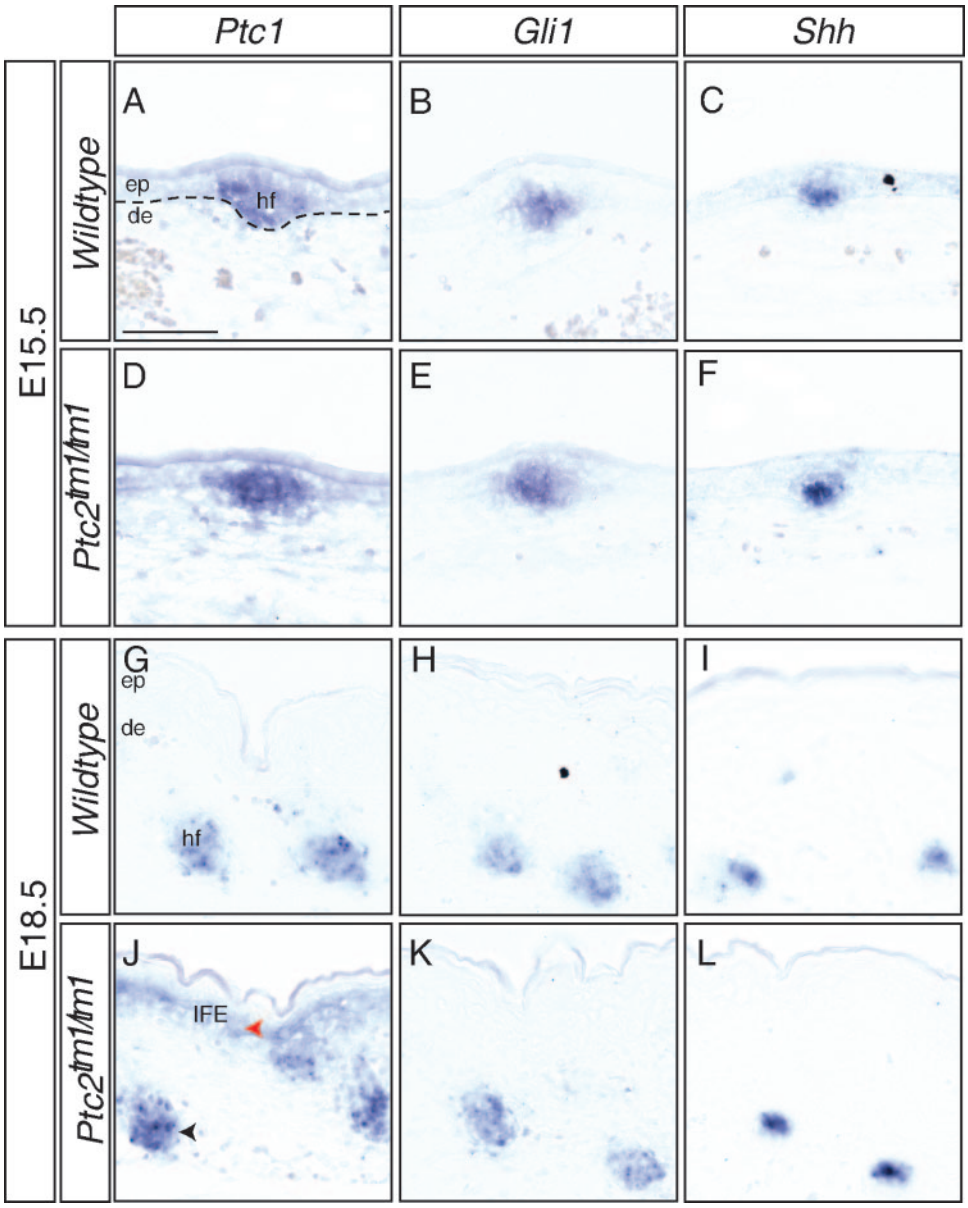

FIG. 6. *Ptc1* is upregulated in *Ptc2*$^{tm1/tm1}$ embryonic skin. Shown is expression of *Ptc1* (A, D, G, and J), *Gli1* (B, E, H, and K), and *Shh* (C, F, I, and L) in wild-type (A to C and G to I) and *Ptc2*$^{tm1/tm1}$ (D to F and J to L) embryos at E15.5 (A to F) and E18.5 (G to L). *Ptc1* is slightly upregulated in E18.5 hair follicles (black arrowhead) and ectopically expressed in the interfollicular epidermis (IFE; red arrowhead) in *Ptc2*$^{tm1/tm1}$ skin. Dashed lines indicate epidermis-dermis boundaries. ep, epidermis; de, dermis; hf, hair follicle. Scale bar: 50 μM.

structures such as hair follicles, and hair follicle development is arrested in *Shh*$^{-/-}$ mice (16, 59). We have previously shown that *Ptc2* and *Shh* are coexpressed in the developing hair follicles during mouse embryogenesis (45). To determine whether *Ptc2* plays a role in hair follicle development, we analyzed E15.5 and E18.5 *Ptc2*$^{tm1/tm1}$ skin. Histological analysis showed that *Ptc2* mutants develop hair follicles with normal morphology and density (Fig. 5A, G, M, and S). Marker gene analysis indicated that the differentiation of epidermal cells appears grossly normal. Similar to wild-type skin (Fig. 5B to E and N to Q), *Ptc2*$^{tm1/tm1}$ skin showed normal expression of *Keratin-17* (Fig. 5H and T) and keratin-14 (Fig. 5I and U) in the basal layer, keratin-10 in the suprabasal layer (Fig. 5J and V), and loricrin in the cornified layer (Fig. 5K and W) of the epidermis. Furthermore, epidermal proliferation of *Ptc2*$^{tm1/tm1}$ skin was also similar to that of wild-type skin, as revealed by the expression pattern (Fig. 5F, L, R, and X) and the number of phospho-histone H3-positive cells (Fig. 5Y). These results indicate that normal *Ptc2* function is not required for embryonic hair follicle development.

We next analyzed whether reduction of *Ptc2* function affects the Shh response in developing skin. In situ hybridization analysis indicated that the expression of *Gli1* (Fig. 6H and K) was not affected, while *Ptc1* (Fig. 6G and J) appeared to be ectopically activated in the interfollicular epidermis of *Ptc2*$^{tm1/tm1}$ skin at E18.5. *Ptc1* also appeared slightly ele-

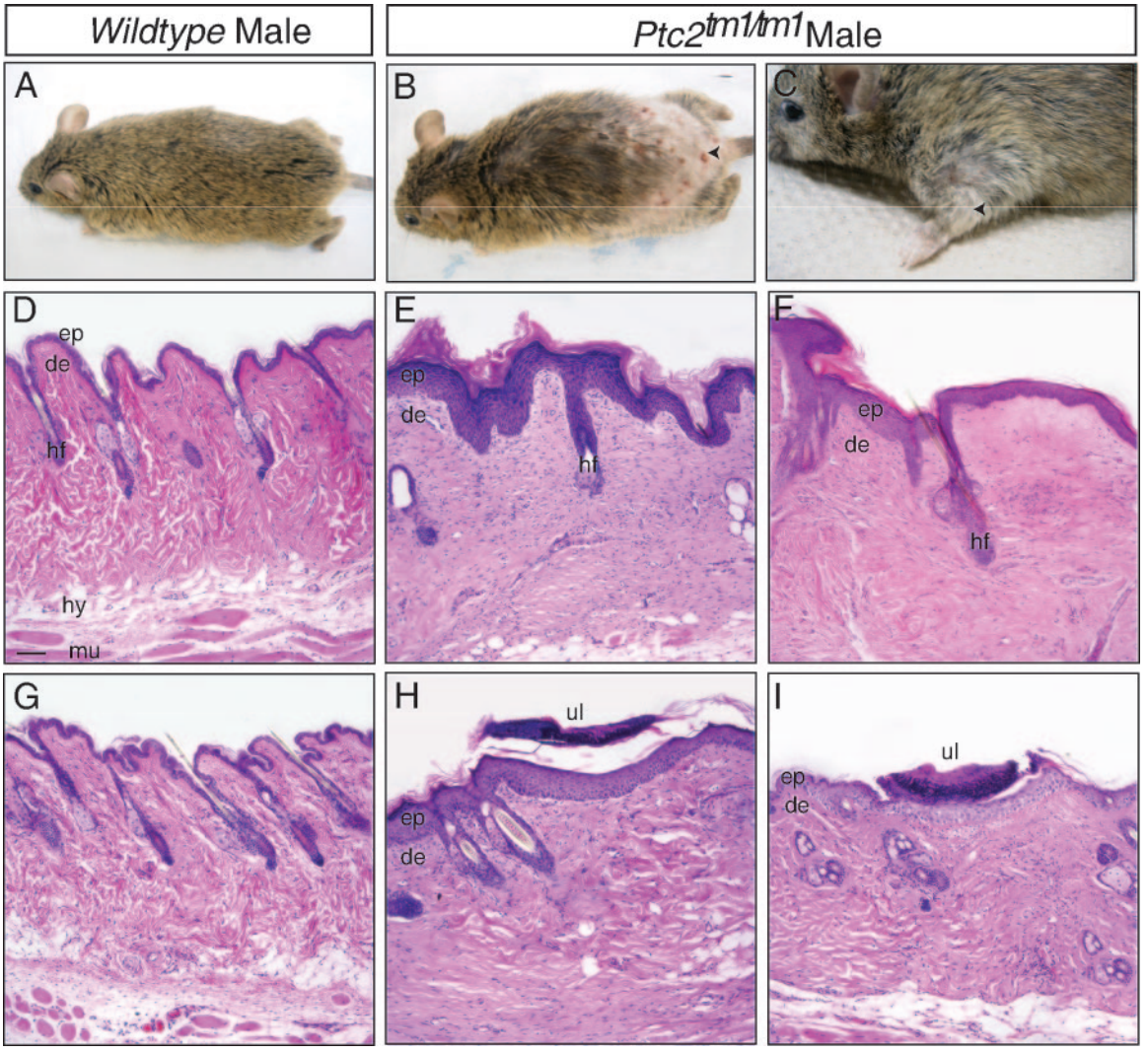

FIG. 7. Ptc2 mutant males develop alopecia and skin lesions. $Ptc2^{tm1/tm1}$ males with ulceration and alopecia on back skin (B) and front paw skin (C) (arrowheads) are shown compared to a normal wild-type male (A). (D and G) Histological staining of wild-type back skin (D) and front paw skin (G). (E and F) Epidermal hyperplasia mutant back skin (E) and front paw skin (F). (H and I) Ulceration shown in mutant back skin (H) and mutant front paw skin (I). ep, epidermis; de, dermis; hf, hair follicle; hy; hypodermis; mu; muscle; ul, ulcer. Scale bar: 50 μM.

vated in E18.5 $Ptc2^{tm1/tm1}$ hair follicles, despite normal follicular expression of *Shh* (Fig. 6C, F, I, and L). Interestingly, hair follicles did not exhibit morphological defects despite ectopic *Ptc1* expression, suggesting that *Ptc1* might be up-regulated as a mechanism to compensate for reduced *Ptc2* function.

Ptc2 mutant males develop alopecia and skin lesions. Despite the lack of an embryonic skin phenotype, 48% of $Ptc2^{tm1/tm1}$

TABLE 1. Phenotypic analysis of adult Ptc2 mutant mice

Phenotype	% of mice					
	Male			Female		
	Wild type (n = 13)	$Ptc2^{tm1/+}$ (n = 38)	$Ptc2^{tm1/tm1}$ (n = 40)	Wild type (n = 12)	$Ptc2^{tm1/+}$ (n = 34)	$Ptc2^{tm1/tm1}$ (n = 50)
Epidermal hyperplasia	0	29	60	0	3	0
Dermal proliferation	0	61	70	0	0	0
Hair follicle loss	0	21	48	0	0	0
Ulcers	0	3	15	0	0	0
Normal	100	26	20	100	97	100

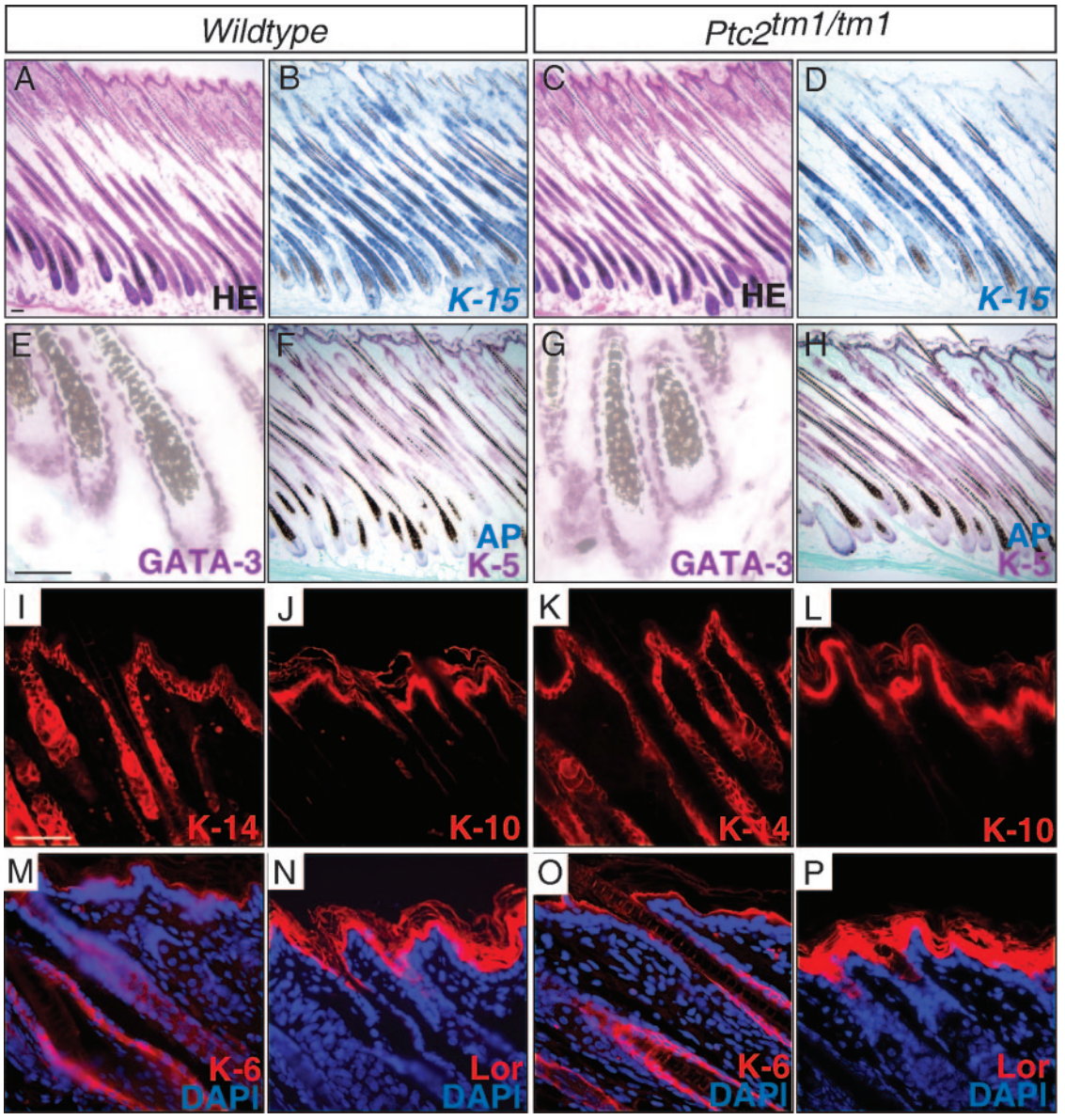

FIG. 8. Hair loss in Ptc2 mutants is not due to aberrant hair follicle development. Shown are histological and immunohistochemical analyses of development of the differentiated layers of the hair follicle and epidermis. (A and C) Normal morphology of hair follicles. All markers analyzed are expressed in the normal pattern. (B and D) Keratin-15 expression in Henle's layer of the IRS; (E and G) GATA-3 is expressed in Huxley's layer of the IRS; (F and G) keratin-5 in the outer root sheath (ORS) and alkaline phosphatase (AP) in the dermal papillae; (M and O) keratin-6 in the companion cell layer. Epidermal development was also normal. (F, H, I, and K) Keratin-5 and keratin-14 in the basal cell layer; (J and L) keratin-10 in the suprabasal layer; (N and P), loricrin (Lor) in the cornified layer. Scale bars: 50 μM. DAPI, 4′,6′diamidino-2-phenylindole; HE, hematoxylin and eosin.

male animals (and $Ptc2^{tm1/+}$ male animals to a lesser extent) develop alopecia (hair loss) and 15% developed spontaneous skin lesions (Fig. 7; Table 1). $Ptc2^{tm1/tm1}$ male animals exhibit an earlier onset of the phenotype (6 to 7 months of age) compared to $Ptc2^{tm1/+}$ male animals (9 to 10 months of age). At 15 months of age, 80% of $Ptc2^{tm1/tm1}$ male animals developed the full spectrum of lesions while 74% of $Ptc2^{tm1/+}$ male animals had lesions (Table 1). Histological analysis of a total of 187 wild-type, $Ptc2^{tm1/+}$, and $Ptc2^{tm1/tm1}$ adult male and female animals (Table 1) revealed that lesions, including epidermal hyperplasia, dermal hyperplasia, hair follicle loss, and ulceration, are observed only in skin samples of $Ptc2^{tm1/+}$ and $Ptc2^{tm1/tm1}$ male animals (Fig. 7E, F, H, and I), but not in those of $Ptc2^{tm1/+}$ and $Ptc2^{tm1/tm1}$ female animals (data not shown). The lesions consistently developed on the dorsal and front paw skin (Fig. 7B and C). We excluded the possibility that these lesions resulted from fighting by housing one male per cage and closely observing them for abnormal grooming behavior.

Since $Ptc2^{tm1/tm1}$ mice developed hair loss, we next wanted to determine whether mutant mice fail to form the appropriate layers of the hair follicle. We performed this study on postnatal day 12 skin since all hair follicles are synchronized in the first

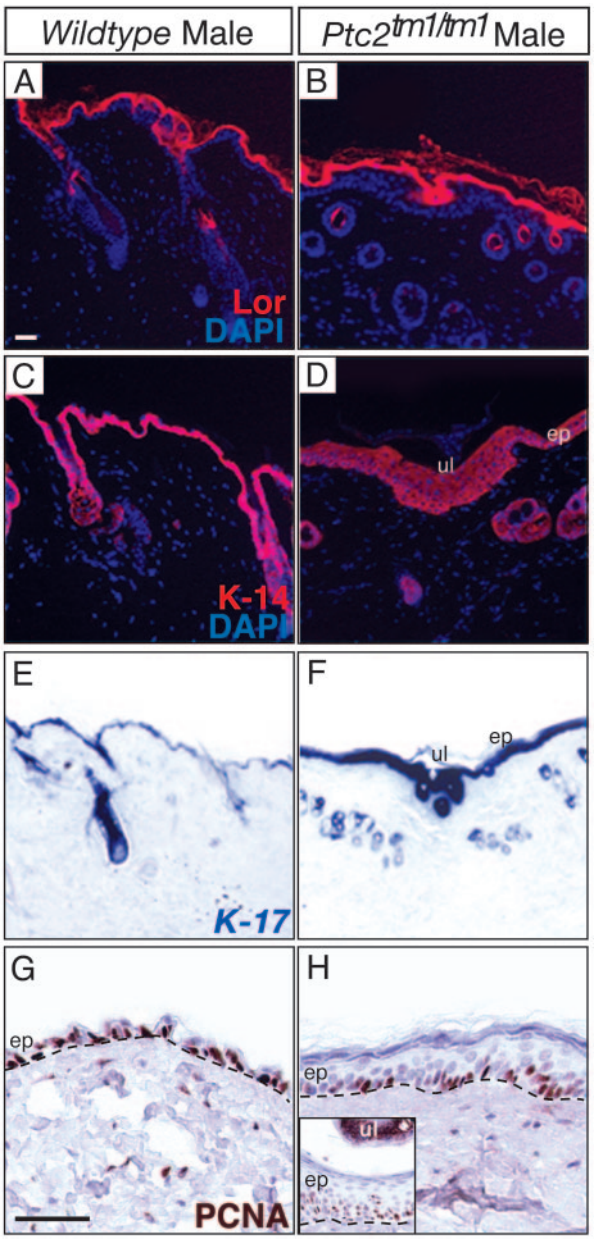

FIG. 9. Marker analysis of skin lesions in Ptc2 mutant males. Shown are immunohistochemistry and in situ hybridization of epidermal compartments. Loricrin (Lor) expression appears to be normal (A and B). Keratin-14 expression is expanded suprabasally in ulcerated *Ptc2*$^{tm1/tm1}$ skin (D) compared to wild-type epidermis, where it is expressed only in the basal layer (C). *Keratin-17* (E and F) expression indicates expansion of the basal layer in areas of epidermal hyperplasia in affected *Ptc2* mutant skin (F). Similar expression of PCNA was observed in wild-type (G) and *Ptc2*$^{tm1/tm1}$ skin (H). Multiple layers of PCNA-expressing cells could be detected in tissue underlying ulcerated lesions (H, inset). ep, epidermis; de, dermis; hf, hair follicle; ul, ulcer. Scale bars: 50 μM.

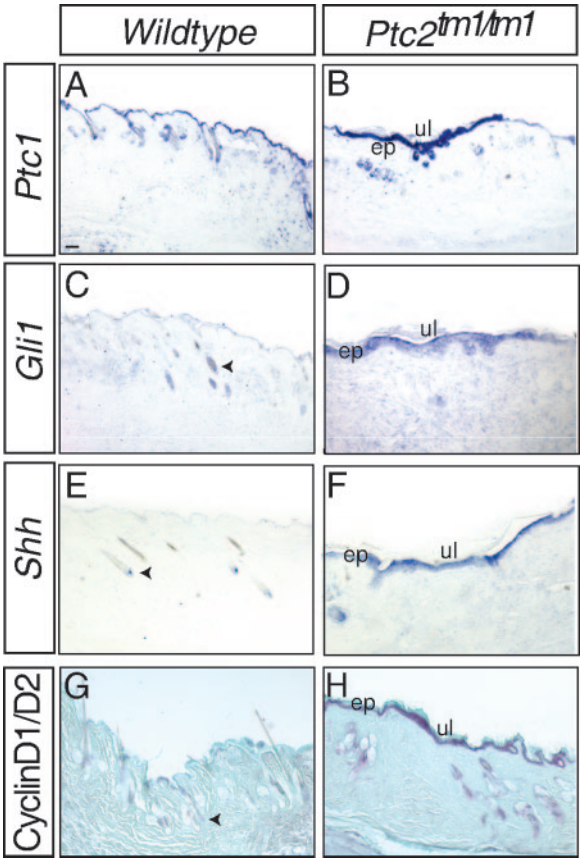

FIG. 10. Sonic hedgehog signaling is activated in the Ptc2$^{tm1/tm1}$ epidermis. Shown is marker gene analysis by in situ hybridization (A to F) and immunohistochemistry (G to H). *Ptc1* (A and B), *Gli1* (C and D), *Shh* (E and F), and cyclin D1/D2 (G to H) expression is increased in areas of epidermal hyperplasia in affected *Ptc2*$^{tm1/tm1}$ skin. Arrowheads indicate low levels of *Gli1*, *Shh*, and cyclin D1/D2 expression in hair follicles of wild-type skin. ep, epidermis; ul, ulcer. Scale bar: 50 μM.

anagen phase of the hair cycle. Histological (Fig. 8A and C) and marker analyses (Fig. 8B and D to P) revealed that the epidermis is normal at this stage. *Keratin-15* expression (Fig. 8B and D) in Henle's layer of the inner root sheath (IRS) was normal. GATA-3 (Fig. 8E and G), a marker for Huxley's layer and the cuticle of the IRS (33), was also expressed in a normal pattern. Keratin-5 (Fig. 8F and H), expressed in the outer root sheath, and keratin-6 (Fig. 8M and O), expressed in the companion cell layer, were expressed similarly in wild-type and mutant samples. We concluded that all the layers of the hair follicles expressed the appropriate markers, suggesting that hair loss in *Ptc2* mutants is not due to failures in forming the inner or outer root sheaths.

To examine the nature of the skin lesions in *Ptc2*$^{tm1/tm1}$ mice, we analyzed the expression of differentiation and proliferation markers of the epidermis. The analysis revealed that the expression of loricrin, which is a marker of the cornified layer, is grossly normal in the *Ptc2* mutant lesions (Fig. 9A and B). High levels of keratin-14 expression in areas of hyperplasia suggest that the hyperplasia is due to an expanded proliferative basal layer (Fig. 9C and D). As expected for adult skin during the repair process, the domain of *Keratin-17* expression is expanded in the suprabasal cells (Fig. 9E and F) and, consistent with epidermal hyperplasia, the proliferative marker PCNA is also expressed at high levels in the suprabasal cells (Fig. 9G and H).

Shh signaling is activated in regions of epidermal hyperplasia in affected skin of Ptc2 mutants. *Ptc1*, *Gli1*, and *Shh* are normally expressed at low levels in adult skin (Fig. 10A, C, and E) but are upregulated in regions of epidermal hyperplasia in *Ptc2* mutants (Fig. 10B, D, and F). Consistent with increased proliferative capacities and Shh signaling, cyclin D1/D2 protein levels are highly elevated in areas of epidermal hyperplasia (Fig. 10G and H). Previous reports indicated that D-type cyclins are involved in Hh-mediated growth control (20, 34, 38, 43, 65), and their upregulation contributes to tumor growth associated with Hedgehog pathway activation (26). These results suggest that the Shh signaling pathway is activated in epidermal hyperplasia associated with the *Ptc2* mutation.

DISCUSSION

***Ptc2^{tm1}* is likely a hypomorphic mutant allele.** The objective of the present study was to elucidate the role of *Ptc2* in mammalian development and Shh signaling. Through targeted insertion of a *neomycin* cassette in exon 6, we have generated *Ptc2^{tm1}* mice. Northern blot and RT-PCR analyses indicated that *Ptc2$^{tm1/tm1}$* mice lack the major *Ptc2* transcript but produce several minor mutant transcripts. We identified a minor splice variant of Ptc2, Ptc2Δ6,7, present in both wild-type and mutant samples. Ptc2Δ6,7 displayed similar subcellular localization as wild-type Ptc2 and possessed only a slightly reduced ability to inhibit Gli-dependent transcription. Previous studies revealed several splice variants for human PTCH2 involving the SSD (52). In our study, alternative splicing appears to affect only regions 5′ to the SSD, revealing a possible difference in the function of mouse and human Ptc2/PTCH2 proteins. Overexpression studies of Ptc2 splice variants resulting from the *Ptc2^{tm1}* mutation suggested that they have a compromised ability to negatively regulate Shh signaling. Taken together, our molecular characterizations suggest that *Ptc2^{tm1}* is likely a hypomorphic mutant allele of *Ptc2*.

Normal Ptc2 function is not essential for embryogenesis. We show here that *Ptc2$^{tm1/tm1}$* mice are viable and fertile and do not display any obvious defects. Although *Ptc2* is expressed in the skin, limb, testes, and cerebellum, our results clearly indicate that reduced *Ptc2* function does not impede embryogenesis, viability, and reproduction. *Ptc2* displays overlapping expression with *Shh* in the epidermal compartment of the developing hair follicles, where *Ptc1* and *Ptc2* show a mostly nonoverlapping expression pattern, suggesting that *Ptc2* might play a unique role during embryonic hair follicle development. Interestingly, in *Ptc2$^{tm1/tm1}$* mutants hair follicle development is not perturbed. There are at least two explanations for the lack of a strong mutant phenotype in *Ptc2$^{tm1/tm1}$* mice. First, *Ptc2$^{tm1/tm1}$* mice might still possess residual *Ptc2* function that is sufficient for programming normal embryonic development. Second, *Ptc1* might compensate for the loss of *Ptc2* function in *Ptc2$^{tm1/tm1}$* mice. As *Ptc1$^{-/-}$* mice die at E9, well before the onset of the major *Ptc2* expression, the latter hypothesis awaits the conditional knockout of *Ptc1* (22) in a *Ptc2* mutant background.

Upregulation of Shh target genes suggests that Ptc2 acts as a negative regulator of Shh signaling. Despite the lack of an apparent mutant phenotype, we can detect a slight upregulation of *Ptc1* and *Gli1* expression in the developing limb buds and hair follicles of *Ptc2$^{tm1/tm1}$* mice, suggesting that, like *Ptc1*, *Ptc2* acts as a negative regulator of Hh signaling. It remains to be determined whether the upregulation of *Ptc1* in *Ptc2$^{tm1/tm1}$* mice contributes to functional compensation. It has been shown that *Ptc2* expression is upregulated in *Ptc1$^{-/-}$* cells and that *Ptc2* expression apparently does not compensate for the lack of *Ptc1* function (6). Interestingly, we also detected upregulation of *Ptc1* expression in the interfollicular epidermis of E18.5 *Ptc2* mutant skin. This finding might suggest that Ptc2 has a specific function in preventing ectopic expression of *Ptc1* in the epidermis.

Ptc2 plays an important role in epidermal homeostasis in mature skin. Interestingly, although adult *Ptc2* mutant mice appear grossly normal, we find that mutant male animals develop skin lesions consisting of alopecia and ulceration with progressing age. These observations indicate that normal *Ptc2* function is required for skin homeostasis and that the phenotype is sex dependent. Histological and marker analysis shows that *Ptc2*-deficient mice have severe epidermal hyperplasia and that the Shh signaling cascade is activated in these lesions. In contrast, cell proliferation and the Shh signaling cascade are not affected in the normal skin of *Ptc2*-deficient mice. Hh pathway activation has been linked to transcriptional activation of cell cycle genes, thus predisposing cells to higher rates of proliferation and hyperplasia. Interestingly, although we have observed Hh pathway activation and upregulation of cyclin D1/D2 expression in the epidermal hyperplasia of *Ptc2*-deficient mice, these lesions never develop into BCC or other skin tumors.

In humans, the etiology and genetic basis of male pattern baldness (androgenetic alopecia) are unclear. Androgenetic alopecia appears to be caused by a combination of genetic predisposition and elevated levels of circulating androgen (21). Normal hair follicles undergo a continuous process of renewal throughout life. In androgenetic alopecia, there is a shortening of the anagen (growth) phase of the hair follicles. Since Shh signaling is required for the initiation of anagen (55), it is possible that epidermal cells lacking normal *Ptc2* function may exhibit a defect in responding to Shh during the adult hair cycle. It is currently unclear why the *Ptc2$^{tm1/tm1}$* phenotype affects only adult males. Intriguingly, it has been reported that, in humans, males heal acute cutaneous wounds more slowly than females and have an altered inflammatory response (2, 3, 63). It has been also demonstrated that the male genotype is a strong positive risk factor for impaired wound healing in the elderly. The mechanisms underlying such sex differences have not been elucidated, although endogenous testosterone has been found to inhibit cutaneous wound healing (4). Interestingly, male gender is also a strong predisposing factor for BCCs in humans and is associated with more BCCs developing per year compared to females (53). In a study of radiation-induced BCCs in *Ptc1* heterozygous mice, only males developed infiltrative BCCs (39). It is possible that BCC development is affected by hormone status and that *Ptc* genes are involved in responses to steroid hormones or their precursors (15).

Is Ptc2 a tumor suppressor? In humans, disease-associated *Ptc1* mutations are dispersed over the entire coding sequence. About three-fourths of them are predicted to result in truncated proteins, while the rest are in-frame insertions and de-

letions. Studies aimed at investigating the effect of Ptc1 missense mutations (6, 7), identified in humans with BCC or NBCCS, suggested that *Ptc1* mutants that had greatly reduced or absent activity might be deficient in maturation and/or endocytosis. No correlation was found between the position of the mutation in the protein sequence and the degree to which Ptc1 function was disrupted, but a mutation in the large extracellular loop blocked Ptc1 maturation and suggested that this loop might be involved in folding or glycosylation. Similarly Ptc2 mutant forms generated in our study also disrupt the large extracellular loop, and from Western blot analysis we predict that Ptc2-Δ5,6 mice have similar defects in maturation. Interestingly, while Ptc2 deletions might affect Ptc2 similarly to missense mutations in Ptc1, $Ptc2^{tm1/tm1}$ mice did not develop tumors.

In this study, we have shown that normal *Ptc2* function is not required for embryogenesis, viability, and reproduction. We speculate that *Ptc1* may be able to compensate for the lack of *Ptc2* function during development; however, *Ptc2* plays an indispensable role in Shh signaling in the adult male mouse skin and is required for skin homeostasis.

ACKNOWLEDGMENTS

We thank S. Yu for technical assistance and A. E. Oro (Stanford University) for providing the $Ptc1^{-/-}$ embryonic fibroblast cells.

E.N. and P.B. were supported through a studentship, fully or in part, by the Ontario Student Opportunity Trust Fund-Hospital for Sick Children Foundation Student Scholarship Program. This work was supported by funds from the National Cancer Institute of Canada to C.-C.H.

REFERENCES

1. **Adolphe, C., M. Narang, T. Ellis, C. Wicking, P. Kaur, and B. Wainwright.** 2004. An in vivo comparative study of sonic, desert and Indian hedgehog reveals that hedgehog pathway activity regulates epidermal stem cell homeostasis. Development **131:**5009–5019.
2. **Ashcroft, G. S., T. Greenwell-Wild, M. A. Horan, S. M. Wahl, and M. W. Ferguson.** 1999. Topical estrogen accelerates cutaneous wound healing in aged humans associated with an altered inflammatory response. Am. J. Pathol. **155:**1137–1146.
3. **Ashcroft, G. S., M. A. Horan, and M. W. Ferguson.** 1998. Aging alters the inflammatory and endothelial cell adhesion molecule profiles during human cutaneous wound healing. Lab Investig. **78:**47–58.
4. **Ashcroft, G. S., and S. J. Mills.** 2002. Androgen receptor-mediated inhibition of cutaneous wound healing. J. Clin. Investig. **110:**615–624.
5. **Aszterbaum, M., A. Rothman, R. L. Johnson, M. Fisher, J. Xie, J. M. Bonifas, X. Zhang, M. P. Scott, and E. H. Epstein, Jr.** 1998. Identification of mutations in the human PATCHED gene in sporadic basal cell carcinomas and in patients with the basal cell nevus syndrome. J. Investig. Dermatol. **110:**885–888.
6. **Bailey, E. C., L. Milenkovic, M. P. Scott, J. F. Collawn, and R. L. Johnson.** 2002. Several PATCHED1 missense mutations display activity in patched1-deficient fibroblasts. J. Biol. Chem. **277:**33632–33640.
7. **Bailey, E. C., L. Zhou, and R. L. Johnson.** 2003. Several human PATCHED1 mutations block protein maturation. Cancer Res. **63:**1636–1638.
8. **Bajestan, S. N., F. Umehara, Y. Shirahama, K. Itoh, S. Sharghi-Namini, K. R. Jessen, R. Mirsky, and M. Osame.** 2005. Desert hedgehog-patched 2 expression in peripheral nerves during Wallerian degeneration and regeneration. J. Neurobiol. **66:**243–255.
9. **Barnes, E. A., M. Kong, V. Ollendorff, and D. J. Donoghue.** 2001. Patched1 interacts with cyclin B1 to regulate cell cycle progression. EMBO J. **20:**2214–2223.
10. **Bellaiche, Y., I. The, and N. Perrimon.** 1998. Tout-velu is a *Drosophila* homologue of the putative tumour suppressor EXT-1 and is needed for Hh diffusion. Nature **394:**85–88.
11. **Briscoe, J., Y. Chen, T. M. Jessell, and G. Struhl.** 2001. A hedgehog-insensitive form of patched provides evidence for direct long-range morphogen activity of sonic hedgehog in the neural tube. Mol. Cell **7:**1279–1291.
12. **Burke, R., D. Nellen, M. Bellotto, E. Hafen, K. A. Senti, B. J. Dickson, and K. Basler.** 1999. Dispatched, a novel sterol-sensing domain protein dedicated to the release of cholesterol-modified hedgehog from signaling cells. Cell **99:**803–815.
13. **Capdevila, J., F. Pariente, J. Sampedro, J. L. Alonso, and I. Guerrero.** 1994. Subcellular localization of the segment polarity protein patched suggests an interaction with the wingless reception complex in *Drosophila* embryos. Development **120:**987–998.
14. **Carpenter, D., D. M. Stone, J. Brush, A. Ryan, M. Armanini, G. Frantz, A. Rosenthal, and F. J. de Sauvage.** 1998. Characterization of two patched receptors for the vertebrate hedgehog protein family. Proc. Natl. Acad. Sci. USA **95:**13630–13634.
15. **Chang-Claude, J., A. Dunning, U. Schnitzbauer, P. Galmbacher, L. Tee, M. Wjst, J. Chalmers, I. Zemzoum, N. Harbeck, P. D. Pharoah, and H. Hahn.** 2003. The patched polymorphism Pro1315Leu (C3944T) may modulate the association between use of oral contraceptives and breast cancer risk. Int. J. Cancer **103:**779–783.
16. **Chiang, C., R. Z. Swan, M. Grachtchouk, M. Bolinger, Y. Litingtung, E. K. Robertson, M. K. Cooper, W. Gaffield, H. Westphal, P. A. Beachy, and A. A. Dlugosz.** 1999. Essential role for Sonic hedgehog during hair follicle morphogenesis. Dev. Biol. **205:**1–9.
17. **Cohen, M. M., Jr.** 2003. The hedgehog signaling network. Am. J. Med. Genet. A. **123:**5–28.
18. **Ding, Q., S. Fukami, X. Meng, Y. Nishizaki, X. Zhang, H. Sasaki, A. Dlugosz, M. Nakafuku, and C. Hui.** 1999. Mouse suppressor of fused is a negative regulator of sonic hedgehog signaling and alters the subcellular distribution of Gli1. Curr. Biol. **9:**1119–1122.
19. **Ding, Q., J. Motoyama, S. Gasca, R. Mo, H. Sasaki, J. Rossant, and C. C. Hui.** 1998. Diminished Sonic hedgehog signaling and lack of floor plate differentiation in Gli2 mutant mice. Development **125:**2533–2543.
20. **Duman-Scheel, M., L. Weng, S. Xin, and W. Du.** 2002. Hedgehog regulates cell growth and proliferation by inducing cyclin D and cyclin E. Nature **417:**299–304.
21. **Ellis, J. A., and S. B. Harrap.** 2001. The genetics of androgenetic alopecia. Clin. Dermatol. **19:**149–154.
22. **Ellis, T., I. Smyth, E. Riley, S. Graham, K. Elliot, M. Narang, G. F. Kay, C. Wicking, and B. Wainwright.** 2003. Patched 1 conditional null allele in mice. Genesis **36:**158–161.
23. **Frohlich, L., Z. Liu, D. R. Beier, and B. Lanske.** 2002. Genomic structure and refined chromosomal localization of the mouse Ptch2 gene. Cytogenet. Genome Res. **97:**106–110.
24. **Goodrich, L. V., L. Milenkovic, K. M. Higgins, and M. P. Scott.** 1997. Altered neural cell fates and medulloblastoma in mouse patched mutants. Science **277:**1109–1113.
25. **Gorlin, R. J.** 1987. Nevoid basal-cell carcinoma syndrome. Medicine (Baltimore) **66:**98–113.
26. **Grachtchouk, V., M. Grachtchouk, L. Lowe, T. Johnson, L. Wei, A. Wang, F. de Sauvage, and A. A. Dlugosz.** 2003. The magnitude of hedgehog signaling activity defines skin tumor phenotype. EMBO J. **22:**2741–2751.
27. **Hahn, H., L. Wojnowski, G. Miller, and A. Zimmer.** 1999. The patched signaling pathway in tumorigenesis and development: lessons from animal models. J. Mol. Med. **77:**459–468.
28. **Hahn, H., L. Wojnowski, A. M. Zimmer, J. Hall, G. Miller, and A. Zimmer.** 1998. Rhabdomyosarcomas and radiation hypersensitivity in a mouse model of Gorlin syndrome. Nat. Med. **4:**619–622.
29. **Hooper, J. E., and M. P. Scott.** 1989. The *Drosophila* patched gene encodes a putative membrane protein required for segmental patterning. Cell **59:**751–765.
30. **Incardona, J. P., J. H. Lee, C. P. Robertson, K. Enga, R. P. Kapur, and H. Roelink.** 2000. Receptor-mediated endocytosis of soluble and membrane-tethered Sonic hedgehog by Patched-1. Proc. Natl. Acad. Sci. USA **97:**12044–12049.
31. **Ingham, P. W., and A. P. McMahon.** 2001. Hedgehog signaling in animal development: paradigms and principles. Genes Dev. **15:**3059–3087.
32. **Karpen, H. E., J. T. Bukowski, T. Hughes, J. P. Gratton, W. C. Sessa, and M. R. Gailani.** 2001. The sonic hedgehog receptor patched associates with caveolin-1 in cholesterol-rich microdomains of the plasma membrane. J. Biol. Chem. **276:**19503–19511.
33. **Kaufman, C. K., P. Zhou, H. A. Pasolli, M. Rendl, D. Bolotin, K. C. Lim, X. Dai, M. L. Alegre, and E. Fuchs.** 2003. GATA-3: an unexpected regulator of cell lineage determination in skin. Genes Dev. **17:**2108–2122.
34. **Kenney, A. M., and D. H. Rowitch.** 2000. Sonic hedgehog promotes G_1 cyclin expression and sustained cell cycle progression in mammalian neuronal precursors. Mol. Cell. Biol. **20:**9055–9067.
35. **Kuwabara, P. E., and M. Labouesse.** 2002. The sterol-sensing domain: multiple families, a unique role? Trends Genet. **18:**193–201.
36. **Lee, Y., H. L. Miller, P. Jensen, R. Hernan, M. Connelly, C. Wetmore, F. Zindy, M. F. Roussel, T. Curran, R. J. Gilbertson, and P. J. McKinnon.** 2003. A molecular fingerprint for medulloblastoma. Cancer Res. **63:**5428–5437.
37. **Lewis, P. M., M. P. Dunn, J. A. McMahon, M. Logan, J. F. Martin, B. St-Jacques, and A. P. McMahon.** 2001. Cholesterol modification of sonic hedgehog is required for long-range signaling activity and effective modulation of signaling by Ptc1. Cell **105:**599–612.
38. **Long, F., X. M. Zhang, S. Karp, Y. Yang, and A. P. McMahon.** 2001. Genetic manipulation of hedgehog signaling in the endochondral skeleton reveals a

direct role in the regulation of chondrocyte proliferation. Development **128:**5099–5108.
39. **Mancuso, M., S. Pazzaglia, M. Tanori, H. Hahn, P. Merola, S. Rebessi, M. J. Atkinson, V. Di Majo, V. Covelli, and A. Saran.** 2004. Basal cell carcinoma and its development: insights from radiation-induced tumors in Ptch1-deficient mice. Cancer Res. **64:**934–941.
40. **Marigo, V., R. A. Davey, Y. Zuo, J. M. Cunningham, and C. J. Tabin.** 1996. Biochemical evidence that patched is the Hedgehog receptor. Nature **384:** 176–179.
41. **Martin, V., G. Carrillo, C. Torroja, and I. Guerrero.** 2001. The sterol-sensing domain of Patched protein seems to control Smoothened activity through Patched vesicular trafficking. Curr. Biol. **11:**601–607.
42. **Mastronardi, F. G., J. Dimitroulakos, S. Kamel-Reid, and A. S. Manoukian.** 2000. Co-localization of patched and activated sonic hedgehog to lysosomes in neurons. Neuroreport **11:**581–585.
43. **Mill, P., R. Mo, H. Fu, M. Grachtchouk, P. C. Kim, A. A. Dlugosz, and C. C. Hui.** 2003. Sonic hedgehog-dependent activation of Gli2 is essential for embryonic hair follicle development. Genes Dev. **17:**282–294.
44. **Mo, R., A. M. Freer, D. L. Zinyk, M. A. Crackower, J. Michaud, H. H. Heng, K. W. Chik, X. M. Shi, L. C. Tsui, S. H. Cheng, A. L. Joyner, and C. Hui.** 1997. Specific and redundant functions of Gli2 and Gli3 zinc finger genes in skeletal patterning and development. Development **124:**113–123.
45. **Motoyama, J., H. Heng, M. A. Crackower, T. Takabatake, K. Takeshima, L. C. Tsui, and C. Hui.** 1998. Overlapping and non-overlapping Ptch2 expression with Shh during mouse embryogenesis. Mech. Dev. **78:**81–84.
46. **Motoyama, J., T. Takabatake, K. Takeshima, and C. Hui.** 1998. Ptch2, a second mouse Patched gene is co-expressed with Sonic hedgehog. Nat. Genet. **18:**104–106.
47. **Mullor, J. L., and I. Guerrero.** 2000. A gain-of-function mutant of patched dissects different responses to the hedgehog gradient. Dev. Biol. **228:**211–224.
48. **Nieuwenhuis, E., and C. C. Hui.** 2005. Hedgehog signaling and congenital malformations. Clin. Genet. **67:**193–208.
49. **Nybakken, K., and N. Perrimon.** 2002. Hedgehog signal transduction: recent findings. Curr. Opin. Genet. Dev. **12:**503–511.
50. **Oro, A. E., K. M. Higgins, Z. Hu, J. M. Bonifas, E. H. Epstein, Jr., and M. P. Scott.** 1997. Basal cell carcinomas in mice overexpressing sonic hedgehog. Science **276:**817–821.
51. **Pearse, R. V., II, K. J. Vogan, and C. J. Tabin.** 2001. Ptc1 and Ptc2 transcripts provide distinct readouts of Hedgehog signaling activity during chick embryogenesis. Dev. Biol. **239:**15–29.
52. **Rahnama, F., R. Toftgard, and P. G. Zaphiropoulos.** 2004. Distinct roles of PTCH2 splice variants in Hedgehog signalling. Biochem. J. **378:**325–334.
53. **Ramachandran, S., A. A. Fryer, T. J. Lovatt, A. G. Smith, J. T. Lear, P. W. Jones, and R. C. Strange.** 2003. Combined effects of gender, skin type and polymorphic genes on clinical phenotype: use of rate of increase in numbers of basal cell carcinomas as a model system. Cancer Lett. **189:**175–181.
54. **Sasaki, H., C. Hui, M. Nakafuku, and H. Kondoh.** 1997. A binding site for Gli proteins is essential for HNF-3β floor plate enhancer activity in transgenics and can respond to Shh in vitro. Development **124:**1313–1322.
55. **Sato, N., P. L. Leopold, and R. G. Crystal.** 1999. Induction of the hair growth phase in postnatal mice by localized transient expression of Sonic hedgehog. J. Clin. Investig. **104:**855–864.
56. **Semevolos, S. A., M. L. Strassheim, J. L. Haupt, and A. J. Nixon.** 2005. Expression patterns of hedgehog signaling peptides in naturally acquired equine osteochondrosis. J. Orthop. Res. **23:**1152–1159.
57. **Shimokawa, T., F. Rahnama, and P. G. Zaphiropoulos.** 2004. A novel first exon of the Patched1 gene is upregulated by Hedgehog signaling resulting in a protein with pathway inhibitory functions. FEBS Lett. **578:**157–162.
58. **Smyth, I., M. A. Narang, T. Evans, C. Heimann, Y. Nakamura, G. Chenevix-Trench, T. Pietsch, C. Wicking, and B. J. Wainwright.** 1999. Isolation and characterization of human patched 2 (PTCH2), a putative tumour suppressor gene in basal cell carcinoma and medulloblastoma on chromosome 1p32. Hum. Mol. Genet. **8:**291–297.
59. **St-Jacques, B., H. R. Dassule, I. Karavanova, V. A. Botchkarev, J. Li, P. S. Danielian, J. A. McMahon, P. M. Lewis, R. Paus, and A. P. McMahon.** 1998. Sonic hedgehog signaling is essential for hair development. Curr. Biol. **8:**1058–1068.
60. **Stone, D. M., M. Hynes, M. Armanini, T. A. Swanson, Q. Gu, R. L. Johnson, M. P. Scott, D. Pennica, A. Goddard, H. Phillips, M. Noll, J. E. Hooper, F. de Sauvage, and A. Rosenthal.** 1996. The tumour-suppressor gene patched encodes a candidate receptor for Sonic hedgehog. Nature **384:**129–134.
61. **Strutt, H., C. Thomas, Y. Nakano, D. Stark, B. Neave, A. M. Taylor, and P. W. Ingham.** 2001. Mutations in the sterol-sensing domain of Patched suggest a role for vesicular trafficking in Smoothened regulation. Curr. Biol. **11:**608–613.
62. **Taipale, J., M. K. Cooper, T. Maiti, and P. A. Beachy.** 2002. Patched acts catalytically to suppress the activity of Smoothened. Nature **418:**892–897.
63. **Taylor, R. J., A. D. Taylor, and J. V. Smyth.** 2002. Using an artificial neural network to predict healing times and risk factors for venous leg ulcers. J. Wound Care **11:**101–105.
64. **Tseng, T. T., K. S. Gratwick, J. Kollman, D. Park, D. H. Nies, A. Goffeau, and M. H. Saier, Jr.** 1999. The RND permease superfamily: an ancient, ubiquitous and diverse family that includes human disease and development proteins. J. Mol. Microbiol. Biotechnol. **1:**107–125.
65. **Yoon, J. W., Y. Kita, D. J. Frank, R. R. Majewski, B. A. Konicek, M. A. Nobrega, H. Jacob, D. Walterhouse, and P. Iannaccone.** 2002. Gene expression profiling leads to identification of GLI1-binding elements in target genes and a role for multiple downstream pathways in GLI1-induced cell transformation. J. Biol. Chem. **277:**5548–5555.
66. **Zaphiropoulos, P. G., A. B. Unden, F. Rahnama, R. E. Hollingsworth, and R. Toftgard.** 1999. PTCH2, a novel human patched gene, undergoing alternative splicing and up-regulated in basal cell carcinomas. Cancer Res. **59:**787–792.